Contribution from the Institut für Anorganische und Analytische Chemie, Johannes-Gutenberg-Universität, D-6500 Mainz, FRG, and Max Planck Institut für Festkörperforschung, Heisenbergstrasse 1, D-7000 Stuttgart 80, FRG

Thermoanalytic Investigations on Mixed Crystals of the Spin-Crossover System $[Fe_xZn_{1-x}(2\text{-pic-}ND_2)_3]Cl_2\cdot EtOD$‡

R. Jakobi, H. Spiering, L. Wiehl, E. Gmelin,† and P. Gütlich*

Received June 19, 1987

The specific heat C_p of the mixed crystals $[Fe_xZn_{1-x}(2\text{-pic-}ND_2)_3]Cl_2\cdot EtOD$ (2-pic-ND_2 = 2-picolylamine with a deuteriated amino group) was measured between 115 and 300 K by differential scanning calorimetry (DSC). A pronounced peak dependent on x in the $C_p(T)$ curves was found at the spin transition ($^1A_1 \leftrightarrow {}^5T_2$) temperature of the iron complex. The temperature dependence of the HS fraction γ was obtained from magnetic susceptibility measurements between 4.2 and 300 K. The spin transition $\gamma(T)$ curves allow a determination of the Gibbs free energy as a function of the temperature and the HS fraction. On the basis of these data an almost quantitative explanation of the peak in the $C_p(T)$ curve is given without introducing further parameters.

1. Introduction

Although the phenomenon of thermally induced high-spin (HS) ↔ low-spin (LS) conversion in transition-metal complexes has been extensively studied, there exist only few thermodynamic measurements on spin-crossover compounds. The first was done by Sorai and Seki, who measured precisely the heat capacity C_p of $[Fe(phen)_2(NCS)_2]$ and $[Fe(phen)_2(NCSe)_2]$ between 13 and 375 K.[1] They also parameterized the $C_p(T)$ curve within the scope of a cooperative domain model for the spin transition. Another attempt of a quantitative interpretation of the C_p anomaly coupled with a HS ↔ LS transition was given for the system $MnAs_{1-x}P_x$ by Krokoszinski et al.,[2] who parameterized the free energy, as proposed by Zimmermann and König.[3] In other works[4-7] only qualitative aspects of the transition enthalpy and entropy are discussed. A surprising result was found for the spin-crossover compound $[Fe(bts)_2(NCS)_2]$, where no peak in the $C_p(T)$ curve was observed.[4] The authors conclude that transition enthalpies are mainly caused by an associated crystallographic phase transition and that the contribution of the spin conversion itself is very small. This, however, is in contradiction to experimental results and thermodynamic considerations given in the present work.

The goal of this paper is to show that an almost quantitative description of the peak in the $C_p(T)$ curve is derived from the Gibbs free energy obtained from the temperature dependence of the HS fraction $\gamma(T)$. A suitable compound for this investigation is the system $[Fe_xZn_{1-x}(2\text{-pic-}ND_2)_3]Cl_2\cdot EtOD$, which forms mixed crystals in the whole concentration range ($0 \le x \le 1$). The compound exhibits no structural phase transition accompanying the spin change, as was shown by X-ray diffraction studies.[8] Deuteriation of the amino and the hydroxy group provides two advantages as compared with the case of the nondeuteriated compounds. First, the spin transition exhibits no anomalies as were found for the nondeuteriated complex, which shows a two-step spin conversion;[9] the latter complicates the theoretical treatment and is not the essential feature of usual spin transitions. Second, the deuteriation shifts the transition temperature $T_{1/2} = T(\gamma=0.5)$ about 15 K to higher temperatures,[10] leading to $T_{1/2}$ = 135 K for the pure iron complex. This was important for the present C_p measurements, where the low-temperature limit of the apparatus used was 115 K.

2. Experimental Section

2.1. Sample Preparation. All preparations were carried out in dry oxygen-free atmosphere (N_2 or Ar). The raw materials $[Fe(2\text{-pic-}ND_2)_3]Cl_2\cdot EtOD$ and $[Zn(2\text{-pic-}ND_2)_3]Cl_2\cdot EtOD$ were prepared according to a procedure previously described.[10] The mixed crystals $[Fe_xZn_{1-x}(2\text{-pic-}ND_2)_3]Cl_2\cdot EtOD$ were grown from EtOD solutions containing the desired amounts of the pure Fe and Zn complexes, by slow evaporation of the solvent in a nitrogen stream. Crystals with a volume up to 3 × 3 × 3 mm^3 were obtained. Their purity was checked by elemental analysis. X-ray fluorescence analysis revealed the actual iron concentrations of the mixed crystals: x = 0.91, 0.78, 0.68, 0.60, 0.46.

2.2. Magnetic Susceptibility Measurements. The magnetic susceptibilities were measured in the temperature range 10–293 K with a Foner type magnetometer equipped with a helium flow cryostat. Polycrystalline samples of weights between 34 and 48 mg were used. The magnetometer was calibrated with $Hg[Co(NCS)_4]$. The HS fraction γ can be calculated from the measured susceptibilities with the following assumptions: (1) the iron complex in the HS state shows a Curie law behavior; (2) the LS state shows a temperature-independent paramagnetism; (3) the diamagnetic part of the susceptibility of the iron complex is equal to the susceptibility of the zinc complex.

2.3. Heat Capacity Measurements. Specific heats were measured at temperatures ranging from 115 to 300 K by differential scanning calorimetry using a DSC-2 instrument (Perkin-Elmer). A sapphire crystal and polycrystalline benzoic acid were employed as heat capacity standards.[11] The calibration factors obtained for both materials differed by less than 2% in the whole temperature range. The temperature scale was calibrated with an accuracy better than 1 K by using the melting points of *n*-pentane, chloroform, and tetrachloromethane. The samples of the spin-crossover compounds, consisting of three to six single crystals, were sealed in aluminum pans. The weights of the samples varied between 25 and 32 mg. All scans were carried out in the heating mode at a rate of 10 K/min.

3. Results

The temperature dependence of the HS fractions γ for the mixed crystals is shown in Figure 1. All compounds exhibit a gradual and complete spin transition; i.e., at low temperatures only the low-spin state is populated (γ = 0) while on going to higher temperatures the population of the high-spin state increases continuously until the HS fraction reaches 1. With decreasing iron concentration the $\gamma(T)$ curve is shifted to lower temperatures and its slope becomes less steep. The transition temperature $T(\gamma=0.5)$ depends nearly linearly on x. This behavior is already known from the nondeuteriated compound and from similar materials, e.g. $[Fe_xZn_{1-x}(2\text{-pic})_3]Cl_2\cdot MeOH$.[12,13]

The results of the heat capacity measurements are shown in Figure 2. No anomalies of C_p were found in the range 200–300 K, where C_p increases almost linearly. Only the temperature interval up to 200 K will be displayed here. A peak is observed in the $C_p(T)$ curve in the spin-crossover region for all compounds except for the pure zinc complex, where no spin transition occurs.

* To whom correspondence should be addressed at Johannes-Gutenberg-Universität.
† Max Planck Institute für Festkörperforschung.
‡ Dedicated to Professor Wolfgang Liptay on occasion of his 60th birthday.

(1) Sorai, M.; Seki, S. *J. Phys. Chem. Solids* **1974**, *35*, 555.
(2) Krokoszinski, H. J.; Santandrea, C.; Gmelin, E.; Bärner, K. *Phys. Status Solidi B* **1982**, *113*, 185.
(3) Zimmermann, R.; König, E. *J. Phys. Chem. Solids* **1977**, *38*, 779.
(4) Kulshreshta, S. K.; Iyer, R. M.; König, E.; Ritter, G. *Chem. Phys. Lett.* **1984**, *110*, 201.
(5) Kulshreshta, S. K.; Iyer, R. M. *Chem. Phys. Lett.* **1984**, *108*, 501.
(6) Kaji, K.; Sorai, M. *Thermochim. Acta* **1985**, *88*, 185.
(7) Kulshreshta, S. K.; Sasikala, R.; König, E. *Chem. Phys. Lett.* **1986**, *123*, 215.
(8) Meissner, E. Doctoral Thesis, Universität Mainz, **1984**.
(9) Köppen, H.; Müller, E. W.; Köhler, C. P.; Spiering, H.; Meissner, E.; Gütlich, P. *Chem. Phys. Lett.* **1982**, *91*, 348.
(10) Gütlich, P.; Köppen, H.; Steinhäuser, H. G., *Chem. Phys. Lett.* **1980**, *74*, 475.
(11) Ginnings, D. C.; Furukawa, G. T. *J. Am. Chem. Soc.* **1953**, *75*, 522.
(12) Sorai, M.; Ensling, J.; Gütlich, P. *Chem. Phys.* **1976**, *18*, 199.
(13) Adler, P.; Wiehl, L.; Meissner, E.; Köhler, C. P.; Spiering, H.; Gütlich, P. *J. Phys. Chem. Solids* **1987**, *48*, 517.

0020-1669/88/1327-1823$01.50/0

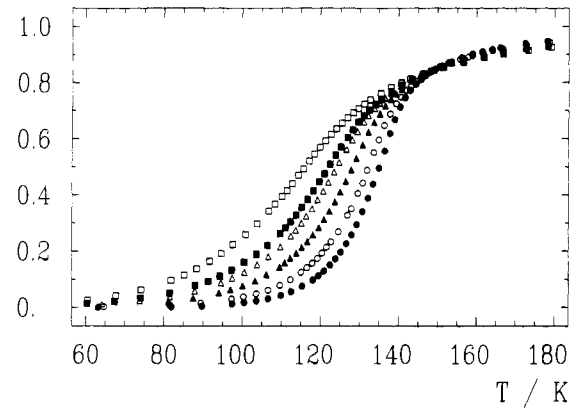

Figure 1. Temperature dependence of the HS fraction in $[Fe_xZn_{1-x}(2\text{-pic-}ND_2)_3]Cl_2\cdot EtOD$ for different iron concentrations: ●, $x = 1.0$; ○, $x = 0.91$; ▲, $x = 0.78$; △, $x = 0.68$; ■, $x = 0.60$; □, $x = 0.46$.

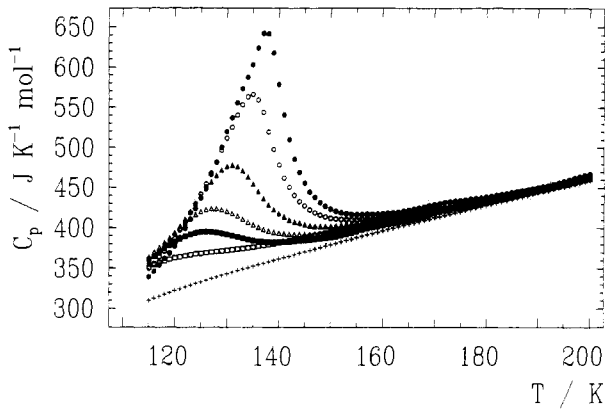

Figure 2. Molar heat capacities of the mixed crystals $[Fe_xZn_{1-x}(2\text{-pic-}ND_2)_3]Cl_2\cdot EtOD$ as functions of temperature: ●, $x = 1.0$; ○, $x = 0.91$; ▲, $x = 0.78$; △, $x = 0.68$; ■, $x = 0.60$; □, $x = 0.46$; +, $x = 0.0$.

The $C_p(T)$ curves depend on the iron content. The peak is shifted to lower temperatures and becomes smaller and broader with decreasing iron concentration.

4. Thermodynamics of the HS ↔ LS Transition

4.1. General Considerations. We assume that the mixed crystals $[Fe_xZn_{1-x}(2\text{-pic-}ND_2)_3]Cl_2\cdot EtOD$ form solid solutions with a random distribution of the HS, LS, and zinc complexes. Regarding the system at constant pressure, the Gibbs free energy per complex molecule g is a function of the temperature T and the relative HS fraction γ:

$$g(T,\gamma) = x[\gamma g_{HS}^{m}(T) + (1-\gamma)g_{LS}^{m}(T) - Ts_{mix}(\gamma) + g_I(\gamma,x,T)] + (1-x)g_{Zn}^{m}(T) + g^{lat}(T) \quad (1)$$

where g_{HS}^{m}, g_{LS}^{m}, and g_{Zn}^{m} refer to the free enthalpy of one isolated HS, LS, and zinc complex molecule. The term g_I describes the interaction between the HS and the LS molecules in the lattice and g^{lat} is the free enthalpy of the lattice per complex molecule. The sum $g_j^{m} + g^{lat}$ will be denoted by g_j, j = HS, LS, Zn, in the following. The mixing entropy is given by

$$s_{mix} = -k_B[\gamma \ln \gamma + (1-\gamma)\ln(1-\gamma)] \quad (2)$$

In thermal equilibrium the HS fraction $\gamma(T)$ is determined by the condition

$$\left(\frac{\partial g}{\partial \gamma}\right)_T = \left[g_{HS} - g_{LS} - k_B T \ln\left(\frac{1-\gamma(T,x)}{\gamma(T,x)}\right) + \frac{\partial g_I}{\partial \gamma}\right] = 0 \quad (3)$$

At very low iron concentrations ($x \sim 0$), the average distance between the iron complexes becomes rather large and the interaction between them can be neglected. In this case the difference of the free enthalpies of the HS and LS molecules Δg can be obtained from the HS fraction

$$\Delta g(T) = g_{HS} - g_{LS} = k_B T \ln\left(\frac{1-\gamma(T,x\sim 0)}{\gamma(T,x\sim 0)}\right) \quad (4)$$

From measurements of $\gamma(T,x)$ and $\gamma(T,x\sim 0)$, the interaction term $\partial g_I(T,x,\gamma)/\partial\gamma$ can be derived according to eq 3.

The molar heat capacity C_p is obtained from the Gibbs free energy by the equation

$$C_p = -N_A T\left(\frac{\partial^2 g}{\partial T^2}\right) \quad (5)$$

where N_A is Avogadro's constant. The first derivative of g with respect to T leads to

$$\frac{\partial g}{\partial T} = x\left[\frac{\partial \gamma}{\partial T}\Delta g + \gamma\frac{\partial \Delta g}{\partial T} - \frac{\partial \gamma}{\partial T}k_B T \ln\left(\frac{1-\gamma}{\gamma}\right) - s_{mix} + \left(\frac{\partial g_I}{\partial \gamma}\right)_T\frac{\partial \gamma}{\partial T} + \left(\frac{\partial g_I}{\partial T}\right)_\gamma + \frac{\partial g_{LS}}{\partial T}\right] + (1-x)\frac{\partial g_{Zn}}{\partial T} \quad (6)$$

This expression contains all terms of eq 3 multiplied by $\partial\gamma/\partial T$. Therefore, the sum of these terms will vanish in equilibrium

$$\frac{\partial g}{\partial T} = x\left[\gamma\frac{\partial \Delta g}{\partial T} - s_{mix} + \left(\frac{\partial g_I}{\partial T}\right)_\gamma + \frac{\partial g_{LS}}{\partial T}\right] + (1-x)\frac{\partial g_{Zn}}{\partial T} \quad (7)$$

And C_p can be written as

$$C_p = -xN_A T\left[\gamma\frac{\partial^2 \Delta g}{\partial T^2} + \frac{\partial \gamma}{\partial T}\left(\frac{\partial \Delta g}{\partial T} + \frac{\partial}{\partial \gamma}\left(\frac{\partial g_I}{\partial T}\right)_\gamma\right) - \frac{\partial s_{mix}}{\partial T} + \left(\frac{\partial^2 g_I}{\partial T^2}\right)_\gamma\right] + xC_p^{LS} + (1-x)C_p^{Zn} \quad (8)$$

where $C_p^{LS} = -N_A T(\partial^2 g_{LS}/\partial T^2)$ and $C_p^{Zn} = -N_A T(\partial^2 g_{Zn}/\partial T^2)$. It should be noted that eq 8 no longer contains the interaction term itself but only its first and second derviatives with respect to temperature.

4.2. Determination of Δg. An essential quantity for the calculation of C_p is the free enthalpy difference of the HS and the LS molecules $\Delta g(T)$. As stated before, it can be derived from the transition curve $\gamma(T,x\sim 0)$ of a highly diluted iron complex. Mössbauer measurements of the relative HS fraction in the temperature range from 40 to 220 K exist for the compound $[Fe_{0.029}Zn_{0.971}(2\text{-pic-}ND_2)_3]Cl_2\cdot EtOD$.[14] At this concentration there may be still a perceptible influence of the interaction. But for the present we will neglect this influence and calculate Δg from eq 4 inserting the $\gamma(T)$ values of the stated compound (Figure 3). For the mixed crystals with higher iron concentrations we determine now $\partial g_I/\partial\gamma$ using eq 3. Figure 4 shows how this expression varies with γ. The resulting curves can be approximately described as straight lines, i.e.

$$\frac{\partial g_I}{\partial \gamma} = A'(x) - 2B'(x)\,\gamma \quad (9a)$$

Figure 5 shows that the slopes B' and the intersections A' depend linearly on x, and so g_I can be written as

$$g_I = Ax\gamma - Bx\gamma^2 + C(x,T) \quad (9b)$$

where $A = A'/x$ (273 cm^{-1}) and $B = B'/x$ (152 cm^{-1}). The term C may depend on x and T, but it is independent of γ. Therefore, it does not appear in the equilibrium condition and has no influence on the spin transition. Equation 9b allows us to calculate the interaction for the complex with the iron concentration $x = 0.029$, and so we can find iteratively a better approximation for Δg. Figure 3 shows the final result, which is already attained by one iteration step. For the calculation of C_p we need further the first

(14) Köppen, H. Doctoral Thesis, Universität Mainz, 1985.

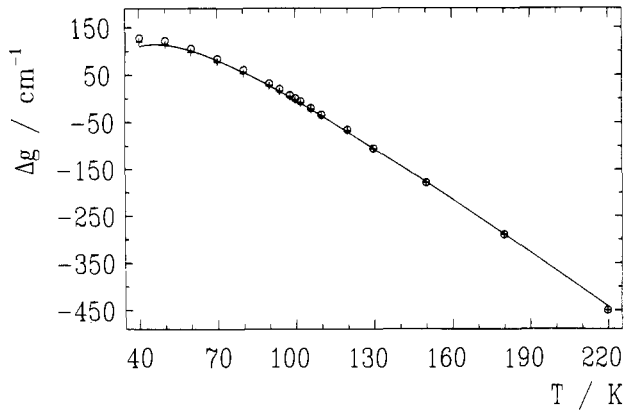

Figure 3. Temperature dependence of the free enthalpy difference of HS and LS molecules: ○, Δg calculated from the HS fraction of $[Fe_{0.029}Zn_{0.971}(2\text{-pic-}ND_2)_3]Cl_2\cdot EtOD$; +, Δg calculated from the HS fraction of $[Fe_{0.029}Zn_{0.971}(2\text{-pic-}ND_2)_3]Cl_2\cdot EtOD$, including the interaction; solid line, Δg fitted as described in the text.

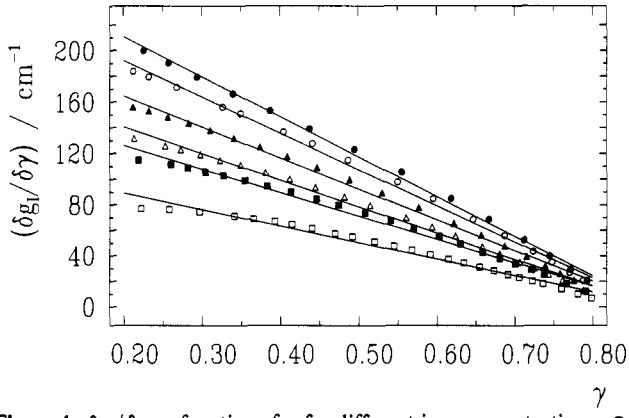

Figure 4. $\partial g_I/\partial\gamma$ as function of γ for different iron concentrations: ●, $x = 1.0$; ○, $x = 0.91$; ▲, $x = 0.78$; △, $x = 0.68$; ■, $x = 0.60$; □, $x = 0.46$.

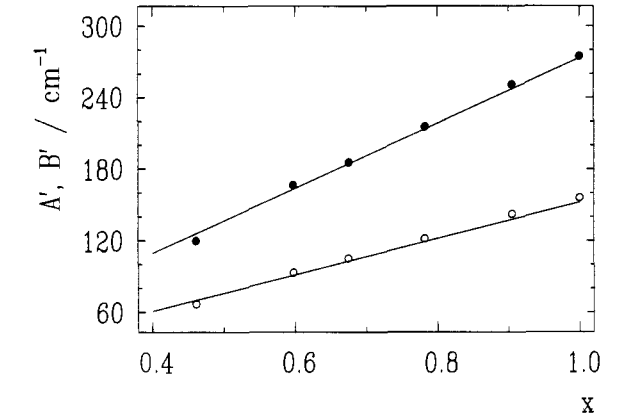

Figure 5. Concentration dependence of A' (●) and B' (○) (eq 9a).

and second derivatives $\partial\Delta g/\partial T$ and $\partial^2\Delta g/\partial T^2$. For the calculation of the derivatives an interpolation between the $\Delta g = g_{HS} - g_{LS}$ values is necessary. Physically the difference between g_{HS} and g_{LS} is mainly caused by the difference of the molecular vibrations.[1] Since in the high temperature limit the specific heat does not depend on the vibrational frequencies, $\Delta C_p = C_p^{HS} - C_p^{LS} = -TN_A(\partial^2\Delta g/\partial T^2)$ must vanish at high temperatures, i.e. $\lim_{T\to\infty} \Delta C_p = 0$. The simplest function for Δg satisfying this condition and leading to an acceptable fit of the experimental Δg values is

$$\Delta g(T) = a + bT + cT^{-1} \tag{10}$$

where a, b, and c are parameters to be fitted. The solid line in Figure 3 is the result of a least-squares fit using eq 10 (a = 486 cm^{-1}, b = 4.04 cm^{-1}/K, c = −8590 cm^{-1} K). Table I shows that

Table I. Difference in Heat Capacities of the High-Spin and Low-Spin Phases at $T_{1/2}$ Derived from C_p Data for Several Compounds That Exhibit a First-Order Transition and the Calculated Value for the Deuteriated Picolylamine Complex

compd	$T_{1/2}$/K	ΔC_p/J K^{-1} mol^{-1}	ref
$[Fe(phen)_2(NCS)_2]$	176.29	18.7	1
$[Fe(phen)_2(NCSe)_2]$	231.26	45.0	1
$[Fe(bt)_2(NCS)_2]$	181.9	45	7
$[Fe(2\text{-pic-}ND_2)_3]Cl_2\cdot EtOD$	135.0	11.3	this work

ΔC_p calculated with these parameters at $T_{1/2}$ yields a reasonable result as compared to corresponding values that were derived from C_p data for other spin-crossover compounds.

It should be noted that the function employed for Δg is equivalent to the phenomenological formula for the free enthalpy proposed by Maier and Kelley[15] if we neglect the terms that vary quadratically or logarithmically with temperature. This may be justified by the fact that we regard here the difference of the free enthalpy of two similar compounds. In the work of Spiering et al.[16] the difference $\Delta g(T)$ for the nondeuteriated compound $[Fe(2\text{-pic})_3]Cl_2\cdot EtOH$ is approximated by a partition function containing electronic energy levels and two estimated effective vibrational frequencies that are different in the HS and the LS state. If this approximation, which requires many more parameters, is used, essentially the same results are obtained.

4.3. Calculation of C_p^{LS}. A direct evaluation of eq 8 is not possible, because the specific heat of the low-spin complex C_p^{LS}, which includes the heat capacity of the lattice, is not known. In the following it will be pointed out that all important information can be obtained if conversely C_p^{LS} is derived from the measured C_p values.

In the approximation of eq 9a the γ-dependent part of g_I does not vary with temperature. Therefore, the corresponding term in eq 8 $\partial/\partial\gamma(\partial g_I/\partial T)$ can be omitted. But the term $-T(\partial^2 g_I/\partial T^2)$ still contains the temperature dependence of the γ-dependent term $C(x,T)$ (eq 9b). This term and C_p^{LS} are the only unknown quantities in eq 8. The sum of these two terms will be denoted as the remaining heat capacity $C_p^R = C_p^{LS} - N_A T(\partial^2 C(x,T)/\partial T^2)$. The specific heat of the LS complex in the spin-crossover region cannot be determined experimentally. For other compounds this quantity was estimated from low-temperature C_p values.[1,6] Corresponding data are not available, but even these data would require an extrapolation over a large temperature range and would therefore lead to uncertain values of C_p^{LS}. If the term C does not depend on x, it can be omitted, because C_p^{LS} formally contains already all temperature-dependent parts of the remaining free enthalpy. In this case we can expect that $C_p^R(T)$ is equal for all mixed crystals and comes out as a smooth and monotonically increasing curve similar to C_p^{Zn}. By the use of eq 8 the remaining heat capacity is given by

$$C_p^R = \frac{1}{x}C_p + N_A T\left[\gamma\frac{\partial^2\Delta g}{\partial T^2} + \frac{\partial\gamma}{\partial T}\frac{\partial\Delta g}{\partial T} - \frac{\partial s_{mix}}{\partial T}\right] - \frac{1-x}{x}C_p^{Zn} \tag{11}$$

Figure 6 shows the calculated C_p^R and, for comparison, the measured C_p values for three different iron concentrations. Similar curves are obtained for the other measurements. Only around $T_{1/2}$ do we still find a very small peak. In the region below and above $T_{1/2}$, where $C_p^R(T)$ is smooth, it is identified with $C_p^{LS}(T)$. The solid line in Figure 6 indicates the mean value $\overline{C_p^{LS}}$ for all mixed crystals, which was fitted as $\overline{C_p^{LS}} = (229 + 1.29T/K - 1.13 \times 10^6 T^{-2}K^2)$ J K^{-1} mol^{-1}.[15] The values around $T_{1/2}$ were excluded for this fit. Except for this region, deviations of C_p^R from the mean value calculated for the different iron concentrations are in general less than 2%. The area $Q = \int(C_p^R - \overline{C_p^{LS}})\,dT$ of the peak around

(15) Maier, C. G.; Kelley, K. K. *J. Am. Chem. Soc.* **1932**, *54*, 3243.
(16) Spiering, H.; Meissner, E.; Köppen, H.; Müller, E. W.; Gütlich, P. *Chem. Phys.* **1982**, *68*, 65.

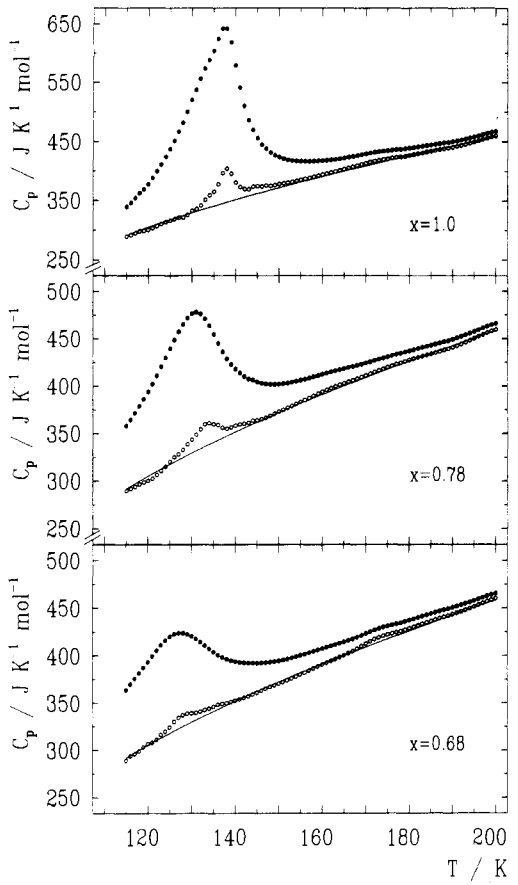

Figure 6. Experimentally determined molar heat capacity of $[Fe_xZn_{1-x}(2\text{-pic-}ND_2)_3]Cl_2\cdot EtOD$ (●) and the remaining specific heat C_p^R (○), which was calculated by subtracting the heat capacity due to the spin transition from the experimental values. C_p^R is essentially equivalent to C_p^{LS}, the specific heat of the low-spin complex. The solid line indicates the mean value of C_p^{LS} for all concentrations, fitted as described in the text.

$T_{1/2}$ is about 5% of the total peak for the pure iron compound and decreases with decreasing iron concentration. At $x = 0.6$ the peak vanishes within the experimental error. The fact that the peak depends on x shows that the term $-T(\partial^2 C(x,T)/\partial T^2)$ cannot be omitted in the temperature region around $T_{1/2}$.

The comparison with the heat capacity of the zinc complex provides another check for the calculated C_p^{LS}. Figure 2 shows that at high temperatures the specific heats of the zinc complex and the iron complex in the HS state, C_p^{HS} and C_p^{Zn}, respectively, are almost equal. Adding to $\Delta C_p(T)$ the average value C_p^{LS}, one obtains the specific heat of the HS compound C_p^{HS} even at low temperatures, where it cannot be measured. The agreement between C_p^{HS} and C_p^{Zn} continues over the whole temperature range. The difference between both quantities is less than 1%.

5. Discussion

The phenomenological description of the thermally induced high-spin ↔ low-spin transition starts with the Gibbs free energy $g(T,\gamma)$ of a solid solution of HS, LS, and other metal complexes (in our case Zn), so that as a first approximation $g(T,\gamma)$ is the sum of the free enthalpies of the complexes and the lattice, in which the complexes are embedded. From the transition curves $\gamma(T,x)$ has been derived the term $g_I(\gamma,x,T)$, which collects all effects of the transition on the lattice and on the complexes themselves. This deviation from a simple noninteracting solid solution is considered as an interaction term. In the "lattice expansion" model of Spiering et al.[16] the term g_I is explained on the basis of an elastic interaction of the complexes, which are of different size in the HS and the LS state. The free enthalpy $g(T,\gamma)$ without the contribution of the molecular and lattice vibrations, which are not affected by the spin change, can be determined completely from the transition $\gamma(T)$ curves. The important result

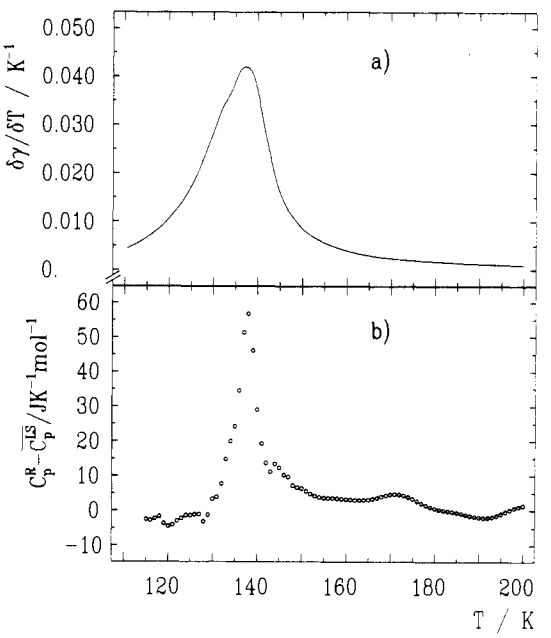

Figure 7. (a) Temperature dependence of the derivative of the HS fraction with respect to temperature, $\partial\gamma/\partial T$, for the pure iron compound. (b) $C_p^R - \overline{C_p^{LS}}$ (for $x = 1$) as a function of temperature.

of the present work is given by the almost quantitative agreement of the measured specific heat with that calculated from $g(T,\gamma)$ curves in the whole temperature range.

It is worth mentioning that this is the first time where such an agreement is obtained without introducing further parameters as in earlier works. Sorai and Seki[1] employed a cooperative domain model and used the C_p data to determine the domain size. Other authors also have used the domain model to interpret high-spin ↔ low-spin transtions.[17] The domain model, however, was in no case specified regarding the underlying physics and was therefore not further pursued. In the work of Krokoszinski et al. the $C_p(T)$ curve was fitted by four parameters including the energy difference of the HS and the LS state and the transition temperature $T_{1/2}$. In the present work all parameters used for the description of $C_p(T)$ were obtained from the free enthalpy, which is completely determined from the transition $\gamma(T)$ curves, and therefore the C_p measurements yield excellent proof for the correctness of the applied form of the free enthalpy.

There remains only a very small peak in the $C_p(T)$ curve that cannot be explained in the employed model. This residual peak attributed to the term $C(x,T)$ cannot be a result of the evaluation procedure. One may argue that not an extra term C but errors in the determination of Δg are responsible for the residual peaks, because $\Delta g(T)$ varies nearly linearly in the corresponding temperature range and therefore small changes lead to an offset in $\partial\Delta g/\partial T$, which results in corrections proportional to $\partial\gamma/\partial T$ according eq 8. However, a comparison of the shapes of two corresponding curves $C_p^R - \overline{C_p^{LS}}$ and $\partial\gamma/\partial T$ as functions of the temperature for the same iron concentration, e.g. for $x = 1$ as displayed in Figure 7, shows that the residual peak cannot be explained by a term that is proportional to $\partial\gamma/\partial T$. For the same reason the term $\partial/\partial\gamma(\partial g_I/\partial T)$ cannot be responsible for the residual peak.

Also, clustering of HS and LS complexes in the transition region or formation of domains, which change the mixing entropy $s_{mix}(\gamma)$ in eq 8, cannot be responsible for the residual peak, because the alteration of s_{mix} should have been corrected by the interaction term $g_I(\gamma,x,T)$, the form of which was determined by the $\gamma(x,T)$ curves. The $\partial g_I(\gamma,x,T)/\partial\gamma$ curves of Figure 4 do not show any peak in the transition region ($\gamma = 0.5$); the curves are smooth over the whole range of γ. Consequently, the missing part of the Gibbs

(17) Gütlich, P.; Köppen, H.; Link, R.; Steinhäuser, H. G. *J. Chem. Phys.* **1979**, *70*, 3977.

free energy that is responsible for this residual peak in the specific heat cannot be obtained from the transition $\gamma(x,T)$ curve.

The fact that the residual peak is just in the transition region where $\partial\gamma/\partial T$ is maximal hints at a small γ-dependent term in the free enthalpy of the compound, which does not influence the shape of the transition $\gamma(x,T)$ curves. We conclude that the missing part of the free energy results from a change in the lattice of the compound that is triggered by the HS $\leftrightarrow$ LS transition. The coupling that would be formally given by a weak γ dependence of $C(x,T,\gamma)$ must be so small that an influence of the HS $\leftrightarrow$ LS transition cannot be observed but large enough to trigger an independent transition in the lattice. The nondeuteriated compound $[Fe(2\text{-pic})_3]Cl_2\cdot EtOH$ shows a pronounced anomaly, i.e. a two-step behavior, in the transition $\gamma(T)$ curve. This case may be an example where the coupling to the inner degrees of freedom of the lattice is strong enough to be observed in the HS $\leftrightarrow$ LS transition.

Acknowledgment. We wish to express our gratitude to the Deutsche Forschungsgemeinschaft, the Fonds der Chemischen Industrie, the Bundesministerium für Forschung und Technologie (Grant No. NT 2723 M), and the Landesgraduiertenförderung Rheinland-Pfalz for financial support. We also wish to thank Professor H. Ringsdorf for allowing us to use his DSC equipment.

Notes

Contribution from the Department of Chemistry, Purdue University, West Lafayette, Indiana 47907

Intervalence Electron Transfer in Bicobaltocene Cations: Comparison with Biferrocenes

George E. McManis, Roger M. Nielson, and Michael J. Weaver*

Received October 8, 1987

As part of a detailed exploration of solvent dynamical effects in electron-transfer reactions, we have recently examined solvent-dependent rate parameters for the self exchange of cobaltocenium/cobaltocene ($Cp_2Co^{+/0}$ where Cp = cyclopentadiene) and for the decamethyl derivative $(Cp\text{-}Me_5)_2Co^{+/0}$ (where $Cp\text{-}Me_5$ = pentamethylcyclopentadiene).[1] A surprising finding from these studies is that the self-exchange rate constant, k_{ex}, in a given solvent is markedly (ca. 10-fold) larger for $Cp_2Co^{+/0}$ and $(Cp\text{-}Me_5)_2Co^{+/0}$ relative to that for the ferrocene analogs, $Cp_2Fe^{+/0}$ and $(Cp\text{-}Me_5)_2Fe^{+/0}$, respectively. Since the nuclear reorganization parameters can be deduced from bond length and vibrational data to be almost identical for the corresponding cobalt and iron systems, these rate differences were traced to dissimilarities in the nature and extent of donor–acceptor orbital overlap.[1b] This interpretation is consistent with the spatial properties of the orbitals involved; thus $Cp_2Fe^{+/0}$ electron exchange appears to employ either an $4e_2$ or $8a_{1g}$ orbital, both of which are strongly metal centered, whereas $Cp_2Co^{+/0}$ exchange apparently utilizes a markedly more ligand-centered $4e_{1g}$ orbital.[1b] The greater facility with which electron exchange occurs for the cobaltocene versus ferrocene systems is attributed to a greater electronic transmission coefficient κ_{el} (i.e., higher electron-tunneling probability within the nuclear transition state) and/or to a correspondingly larger probability of forming reactive precursor complexes with the former reactions.[1b]

Even though this apparent manifestation of donor–acceptor orbital coupling effects in thermal electron transfer is relatively unambiguous, it is desirable to obtain more direct experimental evidence. Such information is readily obtained in suitable cases from the characteristics of optical charge-transfer transitions within mixed-valence complexes.[2] Among the systems of this type that have received detailed experimental scrutiny are biferrocene cations linked by a variety of bridging groups.[3,4] Although the extent of mixed-valence electronic coupling is very sensitive to the structure of the groups linking the metallocene rings, the majority of these systems display near-infrared bands in solution at room temperature that are roughly consistent with so-called "class II" behavior, whereby the optical transition involves electron transfer between valence-trapped metal sites.[3] In this case the extent of donor–acceptor coupling can be treated, at least approximately, by means of Hush theory.[2-6]

Given this favorable picture, we decided to examine the optical properties of analogous mixed-valence bicobaltocene species in order to ascertain if, and to what extent, greater donor–acceptor electronic coupling is indeed engendered in comparison with that for the corresponding biferrocene systems. We selected initially the bicobaltocene cation **1** in view of its simple structure, the availability of a synthetic procedure,[7] and the solvent-dependent intervalence characterization afforded to the biferrocene cation, **2**.[5] The results of this study are presented here. We also compare briefly the optical properties of the corresponding bis(fulvalene)dicobalt and -diiron cations **3** and **4**.

Experimental Section

Acetonitrile, propylene carbonate, dimethylformamide, and methylene chloride were obtained from Burdick and Jackson ("high purity"), and benzonitrile was obtained from Fluka Chemicals. Acetonitrile and methylene chloride were distilled over P_2O_5; the other solvents were used as received. *n*-Tetrabutylammonium hexafluorophosphate (TBAH) was prepared by mixing tetrabutylammonium iodide (Eastman Kodak) and ammonium hexafluorophosphate (Ozark-Mahoning) in acetone and adding water to precipitate the TBAH. It was recrystallized from ethanol.

A solid mixture containing bicobaltocenium(III,III) hexafluorophosphate $[(Cp_2Co)_2(PF_6)_2]$, bis(fulvalene)dicobalt(III,III) hexafluorophosphate, cobaltocenium hexafluorophosphate $[Cp_2CoPF_6]$, and higher order oligomers was prepared using the procedure of Davison and Smart.[7b] We isolated a sample of $(Cp_2Co)_2(PF_6)_2$ by dissolving 1.0 g of the solid mixture in a minimum amount of acetonitrile and passing the solution over a 1.0 × 50 cm column of activated alumina. Elution with acetonitrile yielded four distinct bands; isolation and recrystallization (acetonitrile/ethyl ether) of the material from the second band gave a green powder, determined to be $(Cp_2Co)_2(PF_6)_2$ from the cyclic voltammetry (vide infra) and the proton NMR spectrum.

After $(Cp_2Co)_2(PF_6)_2$ was dissolved in the desired solvent, it was reduced to $(Cp_2Co)_2^+$ by adding an appropriate quantity of cobaltocene

(1) (a) Nielson, R. M.; McManis, G. E.; Golovin, M. N.; Weaver, M. J. *J. Phys. Chem.*, in press. (b) Nielson, R. M.; Golovin, M. N.; McManis, G. E.; Weaver, M. J. *J. Am. Chem. Soc.* **1988**, *110*, 1745.
(2) For a review, see: Creutz, C. *Prog. Inorg. Chem.* **1983**, *30*, 1.
(3) For example: (a) Cowan, D. O.; LeVanda, C.; Park, J.; Kaufman, F. *Acc. Chem. Res.* **1973**, *6*, 1. (b) LeVanda, C.; Bechgaard, K.; Cowan, D. O. *J. Org. Chem.* **1976**, *41*, 2700. (c) Delgado-Pena, F.; Talham, D. R.; Cowan, D. O. *J. Organomet. Chem.* **1983**, *253*, C43. (d) Talham, D. R.; Cowan, D. O. *Organometallics* **1987**, *6*, 932. (e) Talham, D. R.; Cowan, D. O. *Organometallics* **1984**, *3*, 1712.
(4) (a) Cowan, D. O.; LeVanda, C. *J. Am. Chem. Soc.* **1972**, *94*, 9271. (b) Mueller-Westerhoff, U. T.; Eilbracht, P. *J. Am. Chem. Soc.* **1972**, *94*, 9272. (c) LeVanda, C.; Bechgaard, K.; Cowan, D. O.; Mueller-Westerhoff, U. T.; Eilbracht, P.; Candela, G. A.; Collins, R. L. *J. Am. Chem. Soc.* **1976**, *98*, 3181. (d) Kirchner, R. F.; Loew, G. H.; Mueller-Westerhoff, U. T. *Inorg. Chem.* **1976**, *15*, 2665. (e) Mueller-Westerhoff, U. T. *Angew, Chem., Int. Ed. Engl.* **1986**, *25*, 702.
(5) Powers, M. J.; Meyer, T. J. *J. Am. Chem. Soc.* **1978**, *100*, 4393.
(6) (a) Hush, N. S. *Prog. Inorg. Chem.* **1967**, *8*, 391. (b) Hush, N. S. *Electrochim. Acta* **1968**, *13*, 1005.
(7) (a) Smart, J. C. Ph.D. Dissertation, Massachusetts Institute of Technology, Cambridge, MA, 1973, Chapter 3; (b) Davison, A.; Smart, J. C. *J. Organomet. Chem.* **1973**, *49*, C43.

0020-1669/88/1327-1827$01.50/0